NANOPARTICLE FILTRATION IN A RTM PROCESSED EPOXY/CARBON FIBER COMPOSITE

Sandi G. Miller[1], Logan Micham[2], Christine C. Copa[3], Jim M. Criss, Jr.[4], and Eric A. Mintz[5]
[1]NASA Glenn Research Center, Cleveland, OH 44135
[2]NASA LerCIP summer intern, Cleveland, OH 44135
[3]NASA USRP intern, Cleveland, OH. 44135
[4]M&P Technologies, Inc., Marietta GA 30068
[5]Clark Atlanta University, Atlanta, GA 30314

ABSTRACT

Several epoxy matrix composite panels were fabricated by resin transfer molding E862/W resin onto a triaxially braided carbon fiber pre-form. Nanoparticles including carbon nanofiber, synthetic clay, and functionalized graphite were dispersed in the E862 matrix, and the extent of particle filtration during processing was characterized. Nanoparticle dispersion in the resin flashing on both the inlet and outlet edges of the panel was compared by TEM. Variation in physical properties such as T_g and moisture absorption throughout the panel were also characterized. All nanoparticle filled panels showed a decrease in T_g along the resin flow path across the panel, indicating nanoparticle filtration, however there was little change in moisture absorption. This works illustrates the need to obtain good nano-particle dispersion in the matrix resin to prevent particle agglomeration and hence particle filtration in the resultant PMC.

1. INTRODUCTION

RTM is a common processing method for the fabrication of polymer matrix composites.[1] The process uses pressure to force a liquid resin through a preformed reinforcement. When the reinforcement has been fully wet out by the resin, the composite is cured following typical resin cure cycles which include heat and pressure. Nanoparticle dispersion into a resin prior to RTM processing introduces two primary challenges to the fabrication of quality composite parts. The first challenge is increased resin viscosity. Typically, the maximum melt viscosity allowed for RTM processing is between 10 – 30P.[2] An increase in resin viscosity is generally associated with nanoparticle dispersion.[3-5] As a result, only a relatively low nanoparticle loading is possible for RTM. The second processing challenge is the potential for nanoparticle filtration within the reinforcement material if the nano-particles are not fully dispersed. This would lead to a larger nanoparticle loading on the injection side of the part and a lower loading on the outlet side.

Several articles address the issue of nanoparticle filtration.[6-14] Aktas et. al.[6] reported nanoclay clusters were filtered by as much as 50% in the flow direction through a glass pre-form. They also reported, however, that the high shear inherent in RTM processing led to aggregate breakdown and an increased concentration of fine particles at the outlet edge of the panel, relative to the inlet edge.[7] Schlea et. al.[13] optimized CNT dispersion in a thermosetting polyimide (PETI-330) through temperature and shear control, and Criss et. al.[14] describe processing high quality RTM panels from well dispersed PETI-330/CNT nanocomposites.

In this work, three nanoparticles of varying morphology were dispersed in E862 epoxy resin. The E862/W resin system was chosen for this work, as it has been identified as a candidate material for composite engine fan cases and other structures in the fan section of gas turbine engines. A triaxially braided carbon fiber reinforcement was also chosen for its applicability to composite engine structures. The nanoparticles used represent common classes of nano-particulate fillers and included a synthetic clay, an epoxy functionalized nano-graphite, and a carbon nanofiber. Three separate nanocomposite panels were prepared by RTM, as well as a baseline panel composed of only E862 and W curing agent as the matrix. The purpose of this study was to evaluate the extent of nanoparticle filtration throughout a RTM processed nanocomposite matrix panel, and correlate filtration with nanoparticle morphology, dispersion, and composite properties.

2. EXPERIMENTATION

2.1 Materials

Epon 862 epoxy resin and Epikure W curing agent were purchased from Hexion Specialty Chemicals. A triaxially braided carbon fiber preform (HTS40 F13 12K) was received from A&P Technologies. Graphite (Gf): Epoxy coupled graphite was purchased from Adherent Technologies, Inc. The Gf particles were on the order of 50 μm in the lateral dimensions and several stacked graphene sheets in thickness. The surface area of these aggregates was 17 m^2/g; as measured by BET analysis. Synthetic silicate clay(SAP90): Synthetic silicate was received from Claytec, Inc. The particles were composed of individual lamellar sheets, rather than aggregates of stacked sheets. The surface area reported by the manufacturer ranged from 400-700 m^2/g, with the particles averaging 50-100 nm in length. Carbon nanofibers (CNF): PR19-XT-LHT CNFs were purchased from Applied Sciences, Inc. These nanofibers had an average diameter of about 150 nm and a surface area of 15-20 m^2/g; as reported by the manufacturer.

2.2 Nanoparticle dispersion

E862 resin was mixed with the separate nanoparticles at room temperature with a mechanical stirrer over four days. Nanoparticle loading varied based on RTM viscosity limitations. The loading for each particle was used was: SAP90 (2 wt%) CNF (0.5 wt%), and Gf (0.5 wt%). These loadings represent the lower end of a typical nanoparticle loading for each type of material.

2.3 Panel fabrication

E862 (600.3g) and the nanoparticle additive were stirred with EPIKURE W (158.4g) for 5 minutes. The mixture was then loaded into an injector and subsequently plumbed to a flat panel resin transfer molding (RTM) tool. The whole system was put under vacuum and the resin was heated to approximately 120°F (49°C) while the tool was heated to 250°F (121°C). Once at temperature the resin was injected into the RTM tool which contained a braided preform with a $[0]_{3S}$ lay-up. The laminate was then heated to 350°F (177°C) and allowed to cure for 2.5 hours before cooling and de-tooling. The laminate was cured under approximately 200 psi and standard heating and cooling rates for aerospace composites fabrication were used, specifically 3-5°F/min and 5-10°F/min respectively.

2.4 Resin Characterization

Resin flashing from the inlet and outlet panel edges was removed for analysis by scanning electron microscopy (SEM) and transmission electron microscopy (TEM) to characterize nanoparticle dispersion. Differential scanning calorimetry (DSC) of the resin flashing was used to determine T_g on the injection and outlet regions of the panel. Two to three samples were evaluated per material, with a greater number of samples analyzed when there was disparity between the first two runs.

2.5 Composite Characterization

Ultrasonic testing of the samples was accomplished using an immersion scan system manufactured by UTEX Inc. Scans were conducted in a pulse-echo mode with a single 5 MHz transducer acting as both the sender and receiver. C-scan images were generated for each sample based on the amplitude of the ultrasonic wave reflecting from the back surface of the sample. Data was collected at 0.5mm (0.02 in.) in both directions.

Composite panels were cut and samples taken from the inlet side, middle, and outlet regions of the panel. Glass transition temperatures were obtained by Dynamic Mechanical Analysis (DMA/Model No 2980, TA Instruments). Coupon T_g was identified by the peak of the tan δ curve. All samples were cut perpendicular to the axial fiber direction and dried prior to analysis.

Moisture absorption coupons (4"L x1"W) were dried in an air circulating oven at 71^{o}C until the weight change was < 0.01% for two consecutive days. The samples were placed in a humidity chamber at 82^{o}C (180^{o}F)/ 85% humidity. The samples were weighed daily for two and a half weeks (17 days). The edges of the samples were covered with metallic tape to avoid moisture wicking through the cut edge. Five samples were evaluated for each material and an average was taken for the moisture absorption value. Three samples were cut from the middle section of each panel, one from the inlet side, and one from the outlet side.

3. RESULTS

TEM images of nanocomposite samples taken from the inlet and outlet side of each panel are shown at high and low magnification in Figures 1-3. Images from the inlet edge illustrate the extent to which each nanoparticle was dispersed in E862 prior to processing; whereas the outlet edge images serve as a comparison of particulate volume and aggregate size following RTM. The micrographs show aggregation in all cases. Figures 1a and 1b represent the inlet edge of the SAP90 panel, where the individual clay layers were not homogeneously dispersed throughout the resin, but arranged in clusters of exfoliated clay sheets. Along the outlet edge of the SAP90 panel, figures 1c and 1d, a marked reduction in particulate concentration was observed; particularly in at low magnification. A similar degree of dispersion was seen with the CNF, figure 2a and 2b, where aggregates of moderately separated nanofibers were observed in resin taken from the inlet side of the panel. On the outlet side of the CNF panel, figures 2c and 2d, it appears that fewer aggregates passed through the panel, with the outlet edge being composed mostly of single carbon nanofibers. The Gf samples from the inlet side, figure 3a and 3b, were

also inhomogenously arranged in clusters, and within these clusters were smaller aggregates of stacked graphene sheets. As in the previous panels, Gf dispersion at the outlet edge contained smaller aggregates and reduced particle volume relative to the inlet side, figures 3c and 3d.

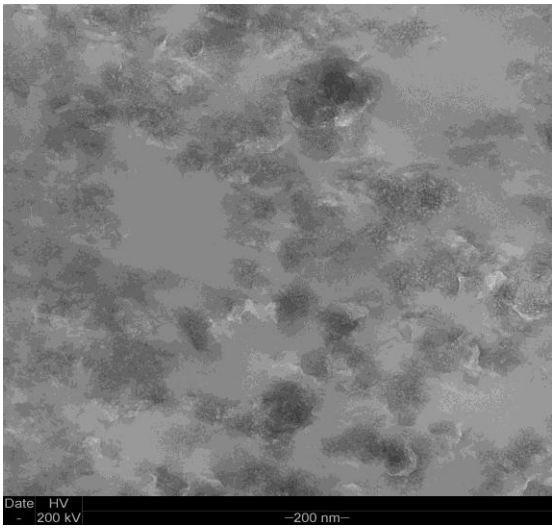

1a

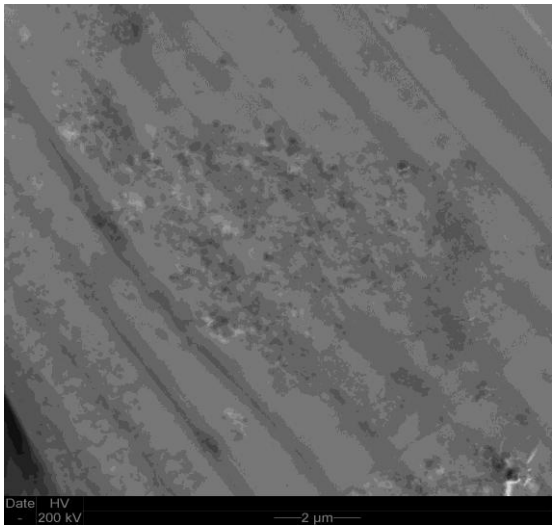

1b

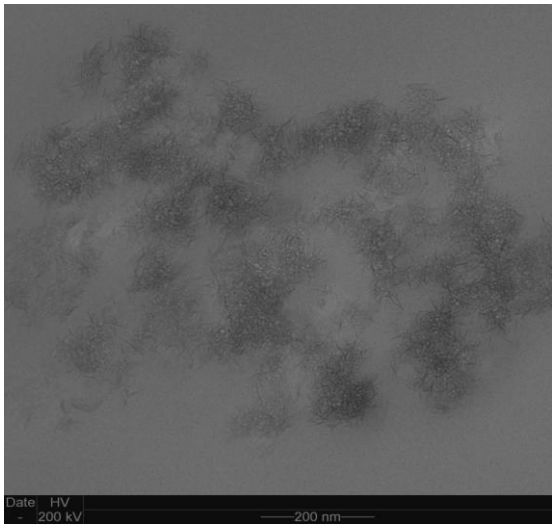

1c

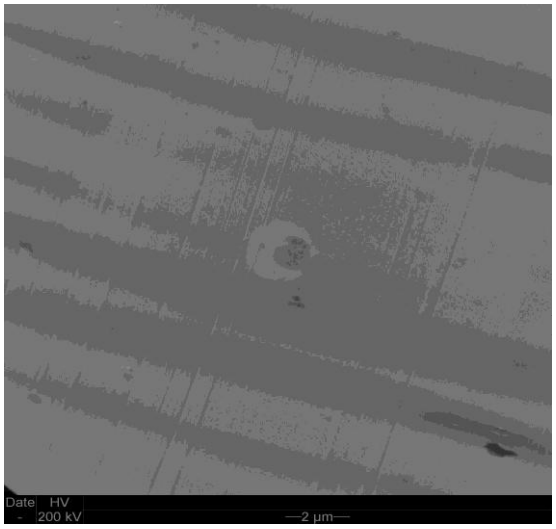

1d

Figures 1a-1b: TEM image of SAP90 in resin along inlet edge at high and low magnification, respectively.
Figures 1c-1d: TEM image of SAP90 in resin along outlet edge at high and low magnification, respectively.

2a 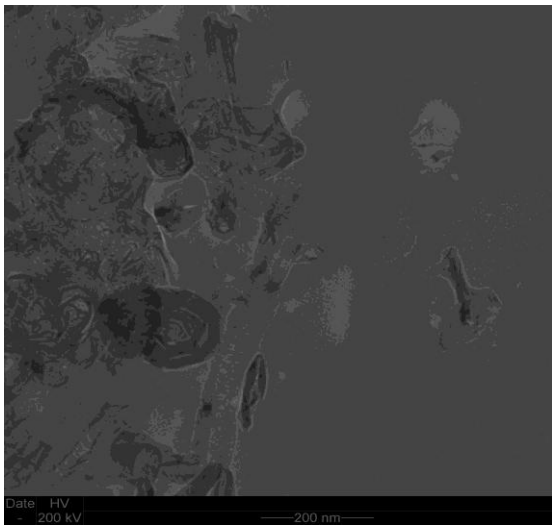

2b 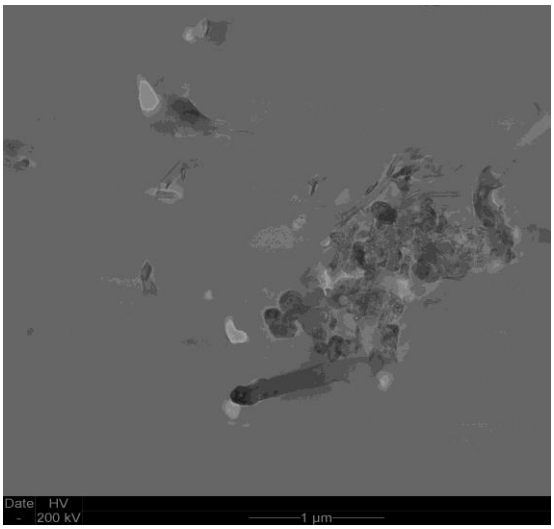

2c 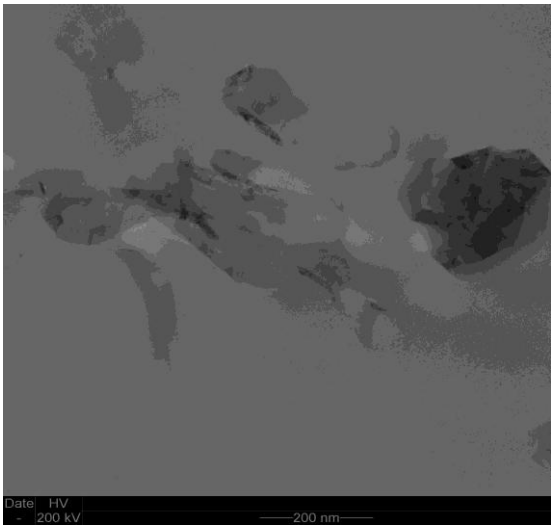

2d 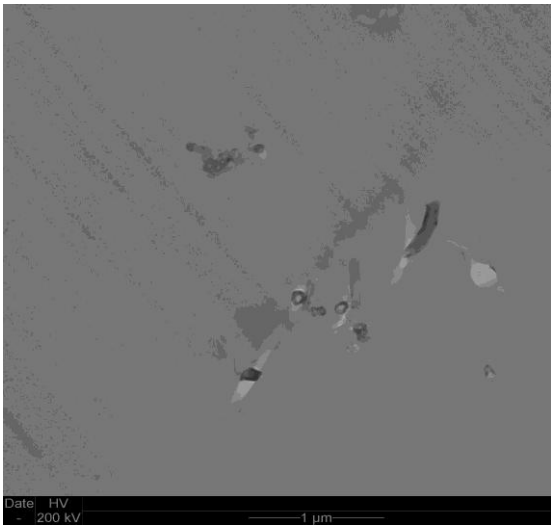

Figures 2a-2b: TEM image of CNF in resin along inlet edge at high and low magnification, respectively.
Figures 2c-2d: TEM image of CNF in resin along outlet edge at high and low magnification, respectively.

3a 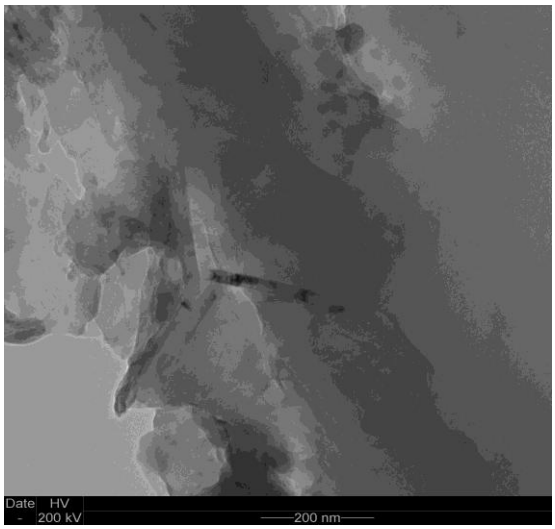

3b 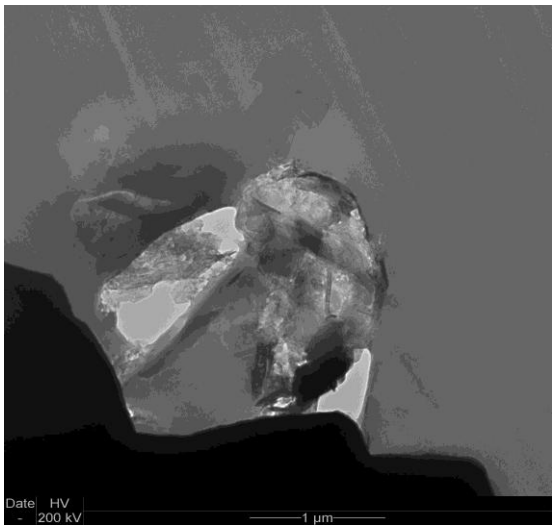

3c 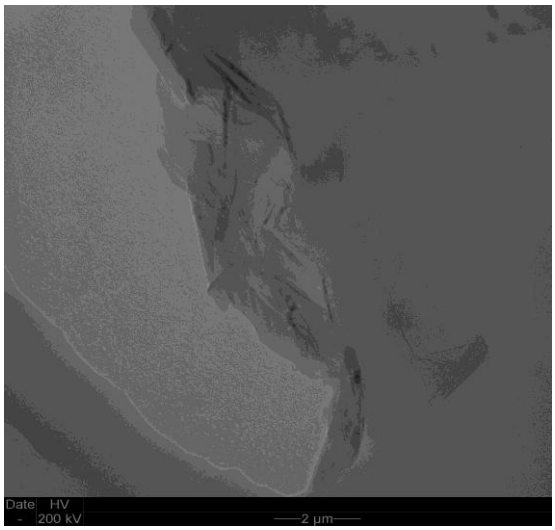

3d 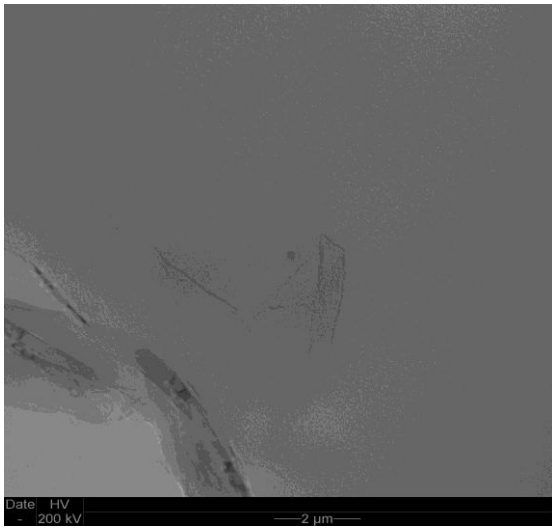

Figures 3a-3b: TEM image of Gf in resin along inlet edge at high and low magnification, respectively.
Figures 3c-3d: TEM image of Gf in resin along outlet edge at low magnification.

The Gf particles were the only nanoparticles which required layer separation from aggregates of stacked sheets. This material proved to be the most difficult to disperse and evidence of particle filtration was immediately visible in the Gf panel. Figure 4 compares the homogenously black flashing along the inlet edge of the Gf panel, and the inhomogeneous dispersion within the resin flashing along the outlet edge. A change in particulate homogeneity was also observed in the CNF panel, however to a lesser extent.

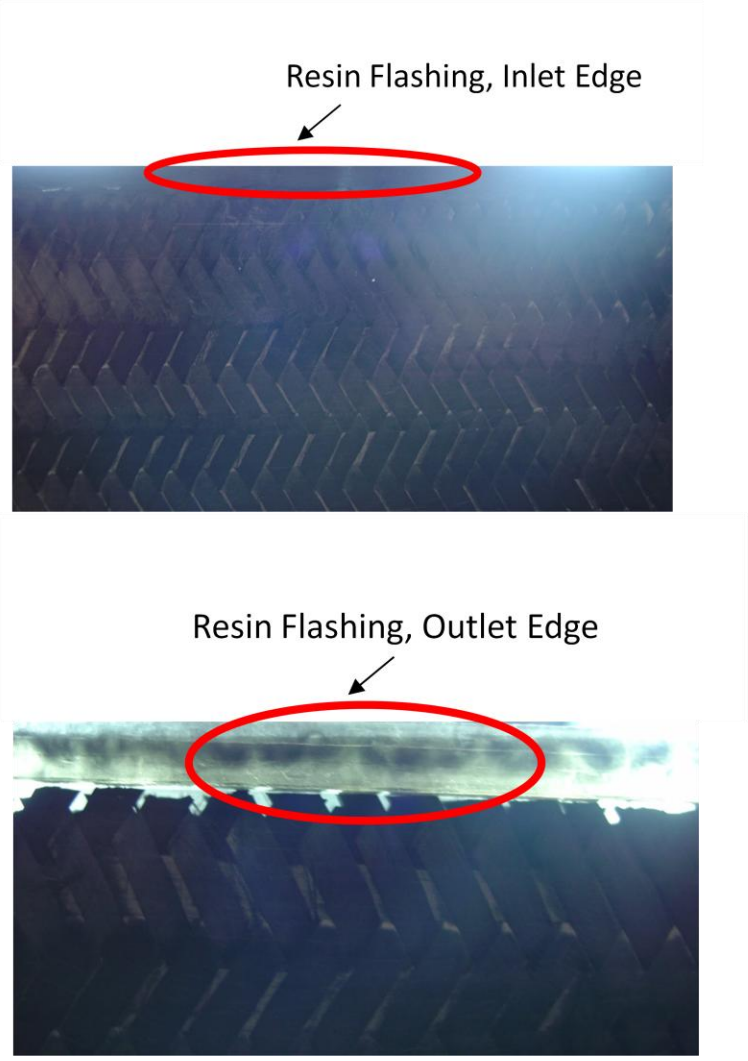

Figure 4: Resin flashing on the outlet edge of the panel containing graphite.

Nanoparticle aggregate size was measured from SEM and TEM images, and these dimensions varied with nanoparticle type. The SAP90 aggregates ranged from 200-400 nm in size. The CNF and Gf aggregates were larger, ranging from 3-5 μm. The aggregate size may become especially critical when a triaxially braided preform is used. The schematic in Figure 5 depicts the triaxially braided fiber with the flow direction identified by the inlet and outlet arrows. The braided architecture imparts an additional 'roadblock' to nanoparticle flow during RTM processing, where resin moving through the preform encounters the axial fibers within each unit cell.

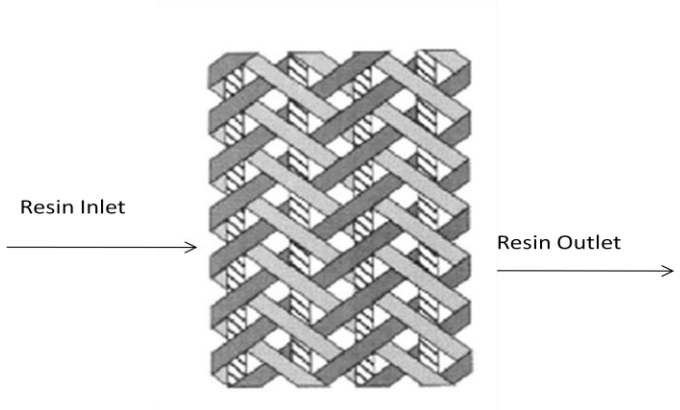

Figure 5: Cartoon of braided fiber.[15]

3.1 Resin Characterization

Table 1 summarizes the DSC characterization of resin flashing at each edge of the nanocomposite panels and shows little change in T_g across the panel, however visual and microscopic analysis point to particulate filtration within each panel during processing. Presumably, there is a prevalence of particulate agglomeration at the inlet edge of the panel with the outlet edge resin predominately composed of dispersed nanoparticles. Filtration would reduce the volume of nanoparticles present along the outlet edge relative to the nanoparticle loading within resin at the inlet edge. Therefore, T_g retention across a nanocomposite panel may infer that the dispersed nano-particles at the outlet side have a greater impact on T_g than the agglomerates at the inlet side. However, T_g retention may also imply that the nanoparticles have no influence on resin T_g. A baseline composite panel had also been prepared for comparison, however, the T_g of the resin dropped from $127^oC \pm 2^oC$ at the inlet side to $105^oC \pm 14^oC$ at the outlet side. It is unclear why the T_g decreased throughout the baseline panel, therefore it was not used for comparison of T_g values.

Table 1: T_g values of resin flashing by DSC

Sample (injection side)	T_g (^oC)	Sample (outlet side)	T_g(^oC)
SAP 90	136 ± 2	SAP 90	139 ± 3
Gf	139 ± 4	Gf	139 ± 4
CNF	139 ± 3	CNF	140 ± 5

3.2 Composite panel characterization

The T_g of the composite was characterized by DMA, where samples were cut from the injection side of the panel, the outlet side, and the middle section to determine that T_g variation. T_g values taken from tan δ peak are shown in Table 2. Within the nanocomposite panels, there was a decrease in T_g across the panel, as would be anticipated with nanoparticle filtration, but was not observed in the resin flashing. The drop in T_g across the SAP90 panel was the greatest while the CNF panel demonstrated the least change in T_g. Mechanical property data will be used to further characterize the influence of particle dispersion and filtration within the nanoparticle filled composite panels.

Table 2: Composite T_g values by tan δ peak from DMA

Sample (injection side)	T_g (°C)	Sample (mid)	T_g (°C)	Sample (outlet side)	T_g(°C)
SAP 90	173	SAP 90	166	SAP 90	162
Gf	172	Gf	170	Gf	166
CNF	168	CNF	166	CNF	162

3.3 Moisture absorption: Filtration and nanoparticle type had minimal influence on moisture absorption into the composite. In general, the weight gain from moisture was small, with the E862 baseline composite gaining only 0.50 wt% over the two and a half week period. The total weight gained for each material is plotted in Figure 6.

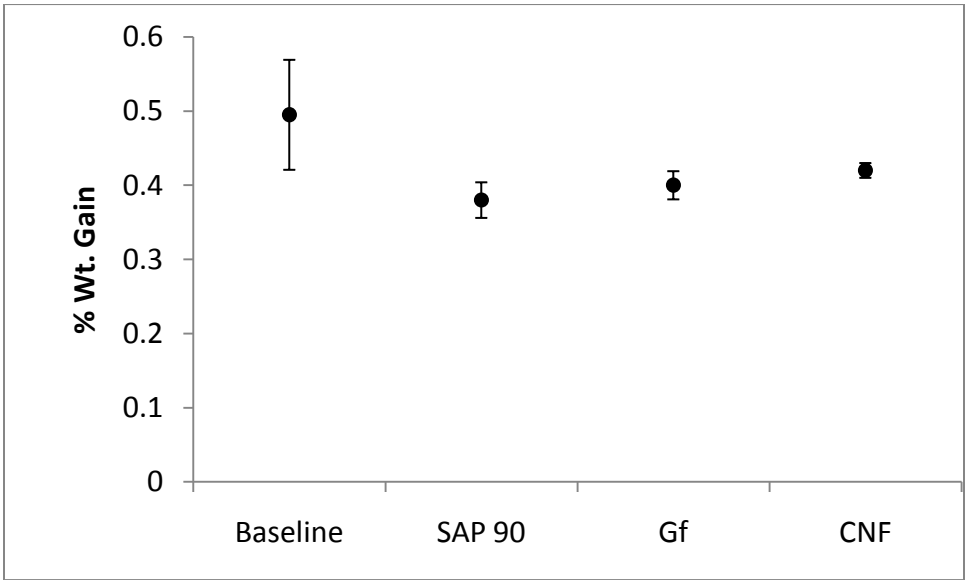

Figure 6: Moisture weight gain baseline and nanocomposite samples.

The data shows that the clay filled laminate gained 25% less moisture than the baseline laminate. The Gf and CNF panels also absorbed 20% and 15% less moisture, respectively, than the neat resin. The platelet morphology of layered silicate clays have typically been associated with improved barrier performance and one would expect that of the three nanoparticles, the clay would have the greatest influence on moisture absorption. The graphite morphology is also a platelet-type and performed well, especially considering the level of visible filtration. The carbon nanofibers presented a barrier to permeation, but because they are fibers rather than platelets, they were nominally less effective at reducing moisture absorption.

4. CONCLUSIONS

A significant level of filtration was observed following RTM processing of nanoparticle filled E862/W resin. The factors that contributed to filtration included (1) poor dispersion, and (2) braid architecture. TEM images of resin taken from the inlet edge of the panel showed aggregation in all nanoparticles and illustrates the need to obtain good dispersions of the nano-particles in order to maximize their affect on the resultant PMC properties. Filtration of the Gf and CNF nanoparticles was evident through visual inspection of the resin flashing along the outlet edge of the panel. The T_g of coupons taken across each nanocomposite panel decreased, which could be due to a gradient in nanoparticle concentration. Moisture absorption into all nanocomposite panels was reduced over 20 percent relative to the baseline resin panel. In this case, the influence of filtration was not evident.

5. ACKNOWLEDGEMENTS

We would also like to acknowledge NASA's Fundamental Aeronautics Program, Supersonics Project for funding.

6. REFERENCES

1. Shojaei, A., Ghaffarian, R., and Karimian, S.M.H., "Modeling and Simulation Approaches in the Resin Transfer Molding Process: A Review", *Polymer Composites* 24 (2003): 525-544.
2. Chuang, K.C., Criss, J.M., and Mintz, E.A., "Polyimides Based on Asymmetric Dianydrides (II) (A-BPDA-ABTDA) for Resin Transfer Molding (RTM), SAMPE 2010 Technical Conference Proceedings, Seattle WA, May 17-20, 2010. CD-ROM- 12pp.
3. Miller, S.G., Bauer, J.L., Marysanski, M.J., Heimann, P.J., Barlow, J.P., Gosau, J.M., and Allred, R.E., "Characterization of Epoxy Functionalized Graphite Nanoparticles and the Physical Properties of Epoxy Matrix Nanocomposites", *Composites Science and Technology* 70 (2010): 1120-1125.
4. Suh, D.J., Lim, Y.T, and Park, O.O., "The Property and Formation Mechanism of Unsaturated Polyester-layered Silicate Nanocomposites Depending on the Fabrication Methods", *Polymer* 41 (2000): 8557-8563.
5. Yudin, V.E., Otaigbe, J.U., Gladchenko, S., Olson, B.G., Nazarenko, S., Korytkova, EN., and Gusarov, V.V., *Polymer* 48 (2007): 1306-1315.
6. Atkas, L., Dharmavaram, S., Hamid, Y.K., and Altan, M.C., *J. Composite Materials* 42 (2008): 2209.
7. Atkas, L., Hamidi, Y.K., and Altan, M.C., "Characterisation of Nanoclay Dispersion in Resin Transfer Moulded Glass/Nanoclay/Epoxy/Composites", *Plastics, Rubbers and Composites* 33 (2004): 267- 272.
8. Khattab, A., Tiamiyu, O., Zhang, P., and Liu, C., "Preliminary Process Investigation of Manufacturing High Temperature Polymer Nanocomposites", SAMPE

9. Sadeghian, R., Gangireddy, S., Minaie, B., and Hsiao, K.-T., "Manufacturing Carbon Nanofibers Toughened Polyester/Glass Fiber Composites Using Vacuum Assisted Resin Transfer Molding for Enhancing the Mode-I Delamination Resistance", *Composites Part A* 37 (2006): 1787-1795.
10. Ghose, S., Watson, K.A., Sun, K.J., Criss, J.M., Siochi, E.J., and Connell, J.W., "High Temperature Resin/Carbon Nanotube Composite Fabrication", *Composites Science and Technology* 66 (2006): 1995-2002.
11. Ware, G., Park, Y.B., Zhang, C., Liang, Z., and Wang, B., "Processing and Characterization of Epoxy/Carbon Fiber/Carbon Nanotube Multiscale Composites Fabricated Using Vartm", SAMPE
12. van Hattum, F.W.J., Leer, C., Carneiro, O.S., "Shear Processing of Carbon Nanofibre composites: Modelling and Characterisation", SAMPE 39th Fall Technical Conference-Cincinnati, OH Oct 29 – Nov 1, 2007.
13. Schlea, M.R., Brown, T.R., Bush, J.R., Criss, J.M., Mintz, E.A., and Shofner, M.L., "Dispersion Control and Characterization in Multiwalled Carbon Nanotube and Phenylethynyl-Terminated Imide Composites," *Composites Science and Technology* 70 (2010): 822-828.
14. Criss, J.M., Powell, W.D., Connell, J.W., Stallworth-Bordain, Y., Brown, T.R., Mintz, E.A., Schlea, M.R., and Shofner, M.L., "Nano-Particle Enhanced Polymer Materials for Space Flight Applications", SAMPE Baltimore May 18-21, 2009.
15. Kelkar, A.D., Tate, J.S., and Bolick, R., "Structural Integrity of Aerospace Textile Composites Under Fatigue Loading", *Materials Science and Engineering B*, 132 (2006): 79-84.